

ANALYSIS OF NONCIRCULAR GEARS MESHING

Marius VASIE, Laurenția ANDREI

”Dunarea de Jos” University of Galati, ROMANIA

v_marius_gl@yahoo.com

ABSTRACT

Based on a general procedure, that uses the supershape equation to generate the pitch curve of the driving gear, and on an analytical approach for the generation of tooth profiles, the paper presents an analysis of the noncircular gear meshing. A first step considers the simulation of rolling, in 2D space, and validates the geometrical and kinematical calculations made in the design phase. Further, the 3D path of contact is analyzed and its distribution and evolution during gears meshing are monitored. Knowing how the path of contact evolves during gear meshing is important for further investigations such as stress and displacement distributions. The lack of researches regarding the meshing conditions of noncircular gears highlights the importance of this paper.

Keywords: noncircular gears, meshing analysis, path of contact

1. INTRODUCTION

Noncircular gears are presented as a curiosity for the gear industry history, due to their complex design and manufacturing difficulties. Nowadays, performant modelling and simulation softwares, advanced CNC machine tools and nonconventional manufacturing technologies enable noncircular gear design and manufacture to be more feasible and to continuously challenge the scientist. As mechanisms used to generate variable motion laws, in comparison with cams, linkages, variable transmission belts, Geneva mechanisms and even electrical servomotors, noncircular gears are remarkable due to their advantages, such as the ability to produce variable speed movements in a simple, compact and reliable way, the lack of gross separation or decoupling between elements, fewer parts in the design phase, the ability to produce high strength-to-weight ratios, etc [1]. The use of noncircular gears in industry certifies their performances, leading to new ideas for improved working conditions.

Generation of noncircular gear is usually developed starting from the hypothesis such as the law of driven gear motion, variation of gear transmission ratio, design of driving gear pitch curve [2-4]. Based on the gear pitch curves, the tooth representation methods consider the theory of envelope surfaces [5], analytical approaches [6] or simulation of the cutting process [7]. Virtual modelling of the noncircular gears, essential for manufacture, could

also be used for further development of a vast theoretical research on meshing conditions, with objectives like path of contact analysis, stress and displacement analysis, the influence of teeth's geometrical parameters and generation and positioning errors of the gears on the gear meshing, etc. From this point of view, the literature is lacunar compared to standard gears, the lack of information being accounted for, perhaps, by the wide range of shapes and materials, lack of standard procedures, etc.

Following the traditional algorithm for noncircular gear generation, the paper briefly presents a general method for the design of gears whose geometry is defined by a constant pressure angle. The main objective of the paper is to investigate the meshing conditions of the designed noncircular gears, highlighting the path of contact evolution and distribution along the teeth placed in the vicinity of the pitch curve minimum radius, where interference could occur and maximum stresses are induced.

2. NONCIRCULAR PITCH CURVES GENERATION

The first step in the noncircular gears virtual design process is the generation of the conjugate pitch curves, starting from a predesigned law of motion for the driven element or a predesigned geometry for the driving gear pitch curve. Based on the second mentioned hypothesis, the authors generalise the driving gear pitch curve by introducing the Gielis' supershape [8], defined by:

$$r_1(\theta_1) = \sqrt{\left| \frac{1}{a} \cdot \cos \frac{n\theta_1}{4} \right|^{n_2} + \left| \frac{1}{b} \cdot \sin \frac{n\theta_1}{4} \right|^{n_3}}^{\frac{1}{n_1}} \quad (1)$$

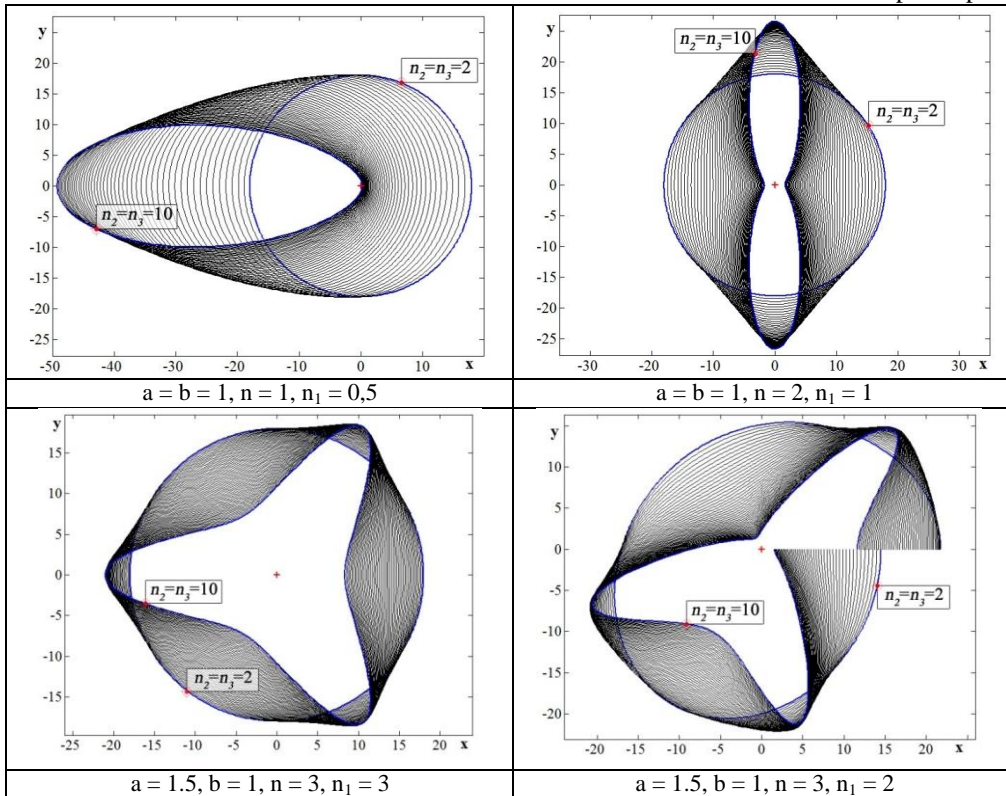
where a , b are non-zero real numbers that define the semi-lengths of the classical ellipse; n - a real number that multiplies the polar angle and defines the number of lobes of the supershape, ie its rotational symmetry; n_1 , n_2 and n_3 - real non-zero numbers that lead to pinched, bloated or polygonal, symmetric or asymmetric shapes, depending on their values and relation.

Table 1 illustrates several families of supershapes, scaled to correspond in length with a standard gear pitch curve defined by modulus $m = 2$ mm and number of teeth $z = 24$. The exponents n_2 , n_3 are considered equal and their variation is chosen as $n_2 = n_3 \in [2, 10]$ (the continuity imposed for the second derivative of the defining function of the supershape, in order to be used in gear theory, requires that exponents n_2 , $n_3 \geq 2$). Other defining parameters are mentioned in Table 1. It can be noticed that for $n_2 = n_3 = 2$, circular pitch curves are obtained; odd number of lobes and different semiaxis lengths lead to open curves; as the exponent n_1 is increased, pitch curve exhibits concave zones and the minimum curvature radius decreases. An extremely versatile curve, the supershape is quite spectacular but it is obvious that, in order to obtain appropriate gear pitch curves, with no pinched or no self-intersecting shapes, with curvatures that exclude the further risk of undercutting during teeth generation, a proper selection of the defining parameters must be done [9].

Once the potential pitch curve geometry is chosen, the next important steps are focused on the determination of the gears center distance and the conjugate pitch curve geometry, respectively. Due to complex equation of the supershape, the determination of the gear center distance, D , is made through numerical integration and iterative procedure, in Matlab environment, and it is based on the assumption that the driving pitch curve performs N_1 revolutions for one revolution of the driven pitch curve and its length is scaled proportionally, to correspond to gear modulus m and number of teeth z_1 .

Closed pitch curves for the driven gears, defined by z_2 number of teeth, are generated if [10]:

Table 1. Families of supershapes



$$\frac{2}{\pi} = \int_0^{2\pi} \frac{1}{m_{12} r_1(\theta_1)} d\theta_1 = \int_0^{2\pi} \frac{r_1(\theta_1)}{r_2(\theta_2)} d\theta_1 = \int_0^{2\pi} \frac{r(\theta)}{D - r_1(\theta)} d\theta_1 \quad (2)$$

where m_{12} is the gear ratio and r_2, θ_2 – the polar coordinate of the driven pitch curve.

The iterative procedure is controlled by an accuracy established at:

$$\Delta = \frac{\pi}{N_1} - \int_0^{2\pi} \frac{r(\theta)}{D - r_1(\theta)} d\theta_1 \leq 10^{-6} \quad (3)$$

Once the gear center distance is obtained, the driven pitch curve can be represented, defined by the following equations:

$$r_2(\theta_2(\theta_1)) = D - r_1(\theta_1) \quad (4)$$

$$\theta_2(\theta_1) = \int_0^{\theta_1} \frac{1}{m_{12}} d\theta_1 = \int_0^{\theta_1} \frac{r(\theta)}{D - r_1(\theta)} d\theta_1 \quad (5)$$

Figure 1 illustrates examples of conjugated noncircular pitch curves, defined by the following common design parameters: the supershape semiaxis lengths $a = 1.5, b = 1$, the gear modulus $m = 2$ mm and the number of revolution of the driving pitch curve $N_1 = 1$. Other specific defined parameters are mentioned in the table.

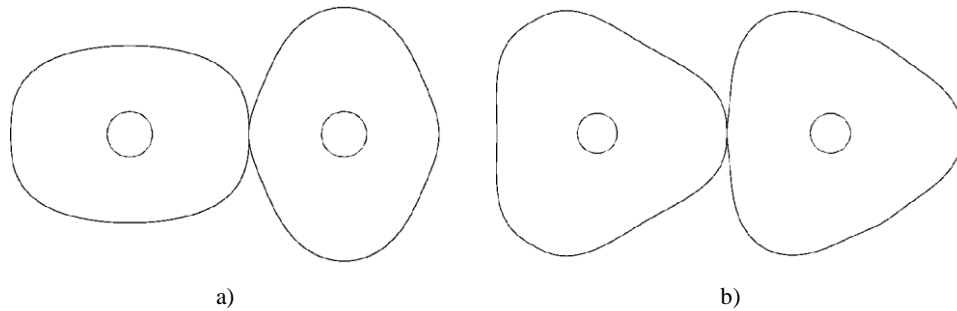


Fig. 1. Examples of conjugated noncircular pitch curves
 a) convex pitch curves ($n = 4, n_1 = 4, n_2 = n_3 = 3, z_1 = 48$)
 b) convex-concave pitch curve ($n = 6, n_1 = 4, n_2 = n_3 = 2.5, z_1 = 60$)

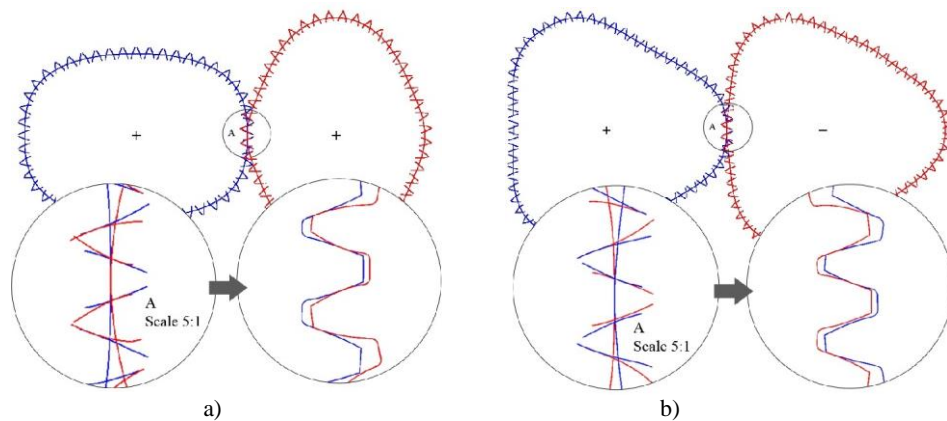


Fig. 2. Tooth profiles of noncircular gears with convex (a) and convex-concave (b) pitch curves

3. TOOTH PROFILES GENERATION

Literature review highlights several methods for noncircular gears' tooth profiles generation, based on analytical procedure, enveloping theory and manufacturing simulation. Considering analytical generation of the gear tooth, the complexity of the pitch curve's defining equation (Eq. 1) requires the development of specific Matlab codes to enable mathematical calculations with a high accuracy.

The analytical generation of the gear tooth flanks, proposed by the authors [11], is based on the rolling movement of one standard rack cutter's tooth over the pitch curve of the noncircular gear. The positioning and rolling of the tool at the level of each tooth satisfy the geometrical and kinematical conditions of gear – rack engagement. After the tooth flanks generation, in Matlab environment, the planar curves are imported, through AutoLISP codes, and edited in AutoCAD, in order to represent the final solid gear model. Fig. 2 illustrates tooth profiles of the gears defined by the pitch curves presented in Fig. 1, with details subtracted from both Matlab and AutoCAD graphic screens.

4. ANALYSIS OF NONCIRCULAR GEARS' MESHING

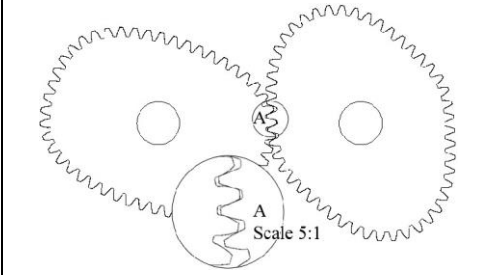
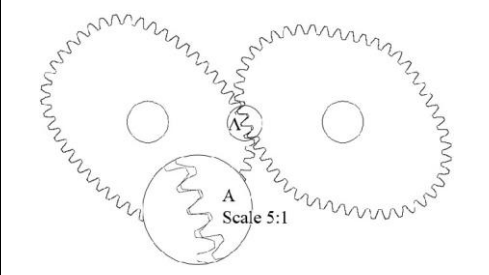
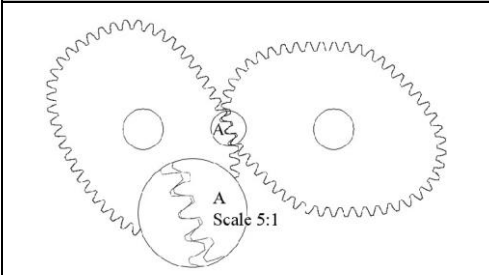
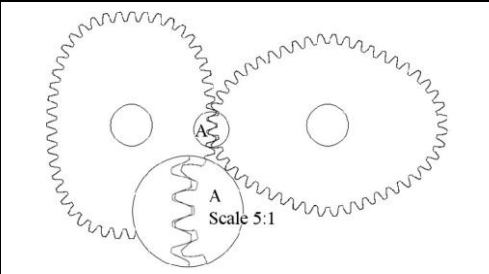
The analysis of the noncircular gear's meshing, in virtual environment, is based on the accuracy and precision of the geometrical and kinematical calculations made in the phase

of tooth profiles generation and aims the engagement simulation and evolution of the gears path of contact.

4.1. Gears' 2D Meshing

An initial check out of the gear tooth profiles generation is developed by the 2D simulation of gears meshing, in AutoCAD environment. Thus, the rotational angle for the driven gear (Eq. 5), calculated through numerical integration in Matlab, is imported to AutoCAD and transmitted to the driven gear while the driving gear perform one revolution. Table 2 captures particular positions of the engagement of one of the two pairs of noncircular gears previously presented (Fig. 2), defined by the following parameters: $a = 1.5$, $b = 1$, $n = 4$, $n_1 = 4$, $n_2 = n_3 = 3$, $m = 2$ mm, $z_1 = 48$, $N_1 = N_2 = 1$. Zooming the meshing zone, no interference could be noticed, even in sensitive zones with smaller curvature radius, certifying that the gear design procedures were properly developed.

Table 2. Noncircular gears' engagement

	
$\theta_1 = 20.01^\circ, \theta_2 = 25.40^\circ$	$\theta_1 = 45.03^\circ, \theta_2 = 54.41^\circ$
	
$\theta_1 = 60.04^\circ, \theta_2 = 67.89^\circ$	$\theta_1 = 90.06^\circ, \theta_2 = 89.97^\circ$

4.2. Gears Path of Contact

The path of contact analysis, performed with solid models of noncircular gears, is necessary for purposes such as: qualitative and quantitative information on teeth engagement and for further studies on the state of stress and displacements. The gears 3D meshing simulation points out the distribution and evolution of the contact between the conjugated tooth flanks. The study is carried out according to the following algorithm:

➤ Starting by defining parameters of the supershape, for a chosen driving gear geometry and kinematics, the tooth profiles of the noncircular gears train are generated in Matlab environment and imported to AutoCAD, where the gear solid models are generated;

➤ On the driving gear, the position of the gear tooth corresponding to the minimum pitch curve radius is chosen to be analyzed (Fig. 3). For this tooth, the angular variation defined by the position of engagement entry and exit points, respectively, is extracted from Matlab results. Six rotational angles are selected, within this variation domain, where the

path of contact is highlighted and investigated, in terms of tooth distribution and corresponding area. It should be specified that the path of contact is figured for a controlled interference, obtained through an additional rotational motion of the driving gear.

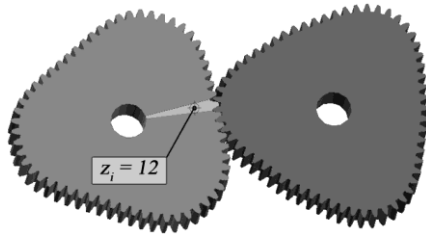


Fig. 3. 3D models of noncircular gears

Table 3. Path of contact for noncircular gears with three lobes

<table border="1"> <tr><td>$A_{z_{i-1}} = 14.46 \text{ mm}^2$</td></tr> <tr><td>$A_{z_i} = 10.08 \text{ mm}^2$</td></tr> <tr><td>$A_{z_{i+1}} = -$</td></tr> </table> <p>$\theta_1 = 52.07^\circ, \theta_2 = 53.95^\circ$</p>	$A_{z_{i-1}} = 14.46 \text{ mm}^2$	$A_{z_i} = 10.08 \text{ mm}^2$	$A_{z_{i+1}} = -$	<table border="1"> <tr><td>$A_{z_{i-1}} = 12.33 \text{ mm}^2$</td></tr> <tr><td>$A_{z_i} = 17.64 \text{ mm}^2$</td></tr> <tr><td>$A_{z_{i+1}} = -$</td></tr> </table> <p>$\theta_1 = 54.57^\circ, \theta_2 = 55.88^\circ$</p>	$A_{z_{i-1}} = 12.33 \text{ mm}^2$	$A_{z_i} = 17.64 \text{ mm}^2$	$A_{z_{i+1}} = -$
$A_{z_{i-1}} = 14.46 \text{ mm}^2$							
$A_{z_i} = 10.08 \text{ mm}^2$							
$A_{z_{i+1}} = -$							
$A_{z_{i-1}} = 12.33 \text{ mm}^2$							
$A_{z_i} = 17.64 \text{ mm}^2$							
$A_{z_{i+1}} = -$							
<table border="1"> <tr><td>$A_{z_{i-1}} = 9.38 \text{ mm}^2$</td></tr> <tr><td>$A_{z_i} = 15.55 \text{ mm}^2$</td></tr> <tr><td>$A_{z_{i+1}} = -$</td></tr> </table> <p>$\theta_1 = 57.08^\circ, \theta_2 = 57.78^\circ$</p>	$A_{z_{i-1}} = 9.38 \text{ mm}^2$	$A_{z_i} = 15.55 \text{ mm}^2$	$A_{z_{i+1}} = -$	<table border="1"> <tr><td>$A_{z_{i-1}} = -$</td></tr> <tr><td>$A_{z_i} = 13.58 \text{ mm}^2$</td></tr> <tr><td>$A_{z_{i+1}} = 16.92 \text{ mm}^2$</td></tr> </table> <p>$\theta_1 = 60.08^\circ, \theta_2 = 60.06^\circ$</p>	$A_{z_{i-1}} = -$	$A_{z_i} = 13.58 \text{ mm}^2$	$A_{z_{i+1}} = 16.92 \text{ mm}^2$
$A_{z_{i-1}} = 9.38 \text{ mm}^2$							
$A_{z_i} = 15.55 \text{ mm}^2$							
$A_{z_{i+1}} = -$							
$A_{z_{i-1}} = -$							
$A_{z_i} = 13.58 \text{ mm}^2$							
$A_{z_{i+1}} = 16.92 \text{ mm}^2$							
<table border="1"> <tr><td>$A_{z_{i-1}} = -$</td></tr> <tr><td>$A_{z_i} = 11.46 \text{ mm}^2$</td></tr> <tr><td>$A_{z_{i+1}} = 17.82 \text{ mm}^2$</td></tr> </table> <p>$\theta_1 = 62.58^\circ, \theta_2 = 61.96^\circ$</p>	$A_{z_{i-1}} = -$	$A_{z_i} = 11.46 \text{ mm}^2$	$A_{z_{i+1}} = 17.82 \text{ mm}^2$	<table border="1"> <tr><td>$A_{z_{i-1}} = -$</td></tr> <tr><td>$A_{z_i} = 5.70 \text{ mm}^2$</td></tr> <tr><td>$A_{z_{i+1}} = 15.96 \text{ mm}^2$</td></tr> </table> <p>$\theta_1 = 65.09^\circ, \theta_2 = 63.86^\circ$</p>	$A_{z_{i-1}} = -$	$A_{z_i} = 5.70 \text{ mm}^2$	$A_{z_{i+1}} = 15.96 \text{ mm}^2$
$A_{z_{i-1}} = -$							
$A_{z_i} = 11.46 \text{ mm}^2$							
$A_{z_{i+1}} = 17.82 \text{ mm}^2$							
$A_{z_{i-1}} = -$							
$A_{z_i} = 5.70 \text{ mm}^2$							
$A_{z_{i+1}} = 15.96 \text{ mm}^2$							

Table 3 presents the evolution of the contact path of the noncircular gear presented in Fig. 3. Tooth number $z_i = 12$ corresponds to the minimum radius of the pitch curve, it has the active flank defined by the angular interval $\theta_1 \in [52.07^\circ, 65.09^\circ]$ and receives an

additional rotation of 0.011° . It was found that there are always two teeth in contact. The tooth starts the engagement with an area of the contact pattern of 9.34 mm^2 , reaches the maximum value of 14.87 mm^2 , in the fifth rotational position, after a rotation of 62.58° for the pinion and 61.96° for the driven gear, leaving the engagement with a minimum value of the contact pattern of 5.70 mm^2 .

4.3. Influence of Supershape Defining Parameters on Gear Path of Contact

It is obvious that each supershape defining parameter, influencing the gear pitch curve geometry, will influence the characteristics of the gear path of contact. A brief study of the noncircular gear meshing, of the design hypothesis above mentioned by the authors, is further developed, the main objective being the proper choice of the potential parameter that would lead to an enhanced gear power transmission capacity.

Figure 4 illustrates the influence the pitch curve number of lobes (n) has on the area of the path of contact monitored on the tooth placed on the minimum curvature radius. The gear train is defined by $a = b = 1$, $n_1 = 1$, $n_2 = n_3 = 3$, $m = 2$, $z = 54$, $N_1 = N_2 = 1$ and the controlled interference is 0.015° . It could be noticed that:

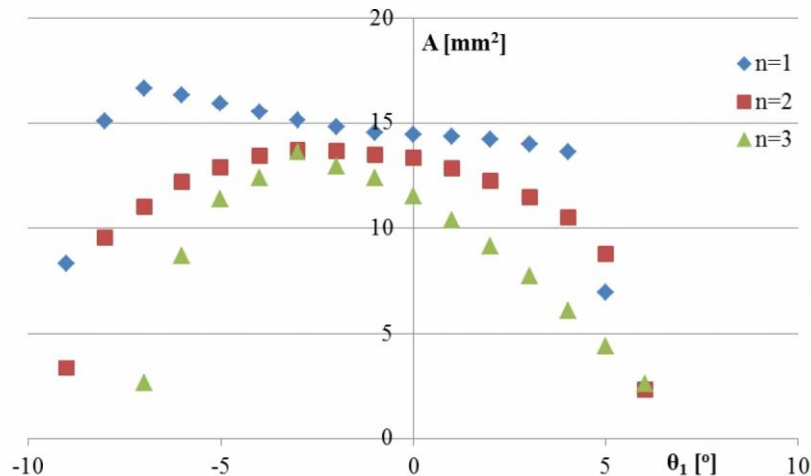


Fig. 4. Evolution of the gear path of contact for gears with one, two and three lobes

- for $n = 1$, the tooth gets into meshing after the pinion is rotated at -9.0251° (rotation in clockwise direction), recording an area of the path of contact of 8.3335 mm^2 , gets the maximum surface contact (16.6859 mm^2), at $\theta_1 = -7.0195^\circ$, and leaves the meshing at $\theta_1 = 5.0139^\circ$, with a contact of 6.9412 mm^2 ;

- for $n = 2$, at starting meshing point, the contact path area is recorded 3.3589 mm^2 , reaches the maximum area of 13.6959 mm^2 and decreases to 2.3192 mm^2 when the tooth flank is about to leave the meshing. The gears contact occurs during the pinion rotational angle $\theta_1 \in [-3.0083^\circ, 6.6221^\circ]$;

- for $n = 3$, the tooth contact increases from the starting area of 2.6458 mm^2 to maximum 13.6056 mm^2 and decreases to 2.5945 mm^2 at contact exit points.

So, as the number of lobes of the driving gear pitch curve is increased, the tooth is engaged along a shorter rotational angle and the area of the contact path is decreased.

Figure 5 illustrates the evolution of the gear path of contact for noncircular gears that varies in pitch curve geometry due to the main exponents n_1 (the designed parameters are: a

($a = b = 1, n = 4, n_2 = n_3 = 3, m = 2$ și $z = 54$). For the same defined interference of 0.015° , it is noticed that an increase in n_1 , even if it reduces the concavity of the pitch curves, does not significantly influence the area of the tooth path of contact, and slightly reduces the contact rotational angle.

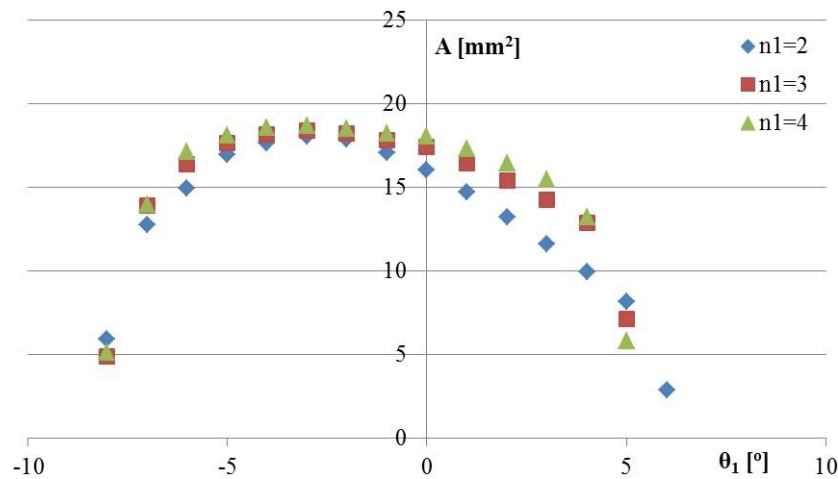


Fig. 5. Influence of exponent n_1 on the gear path of contact

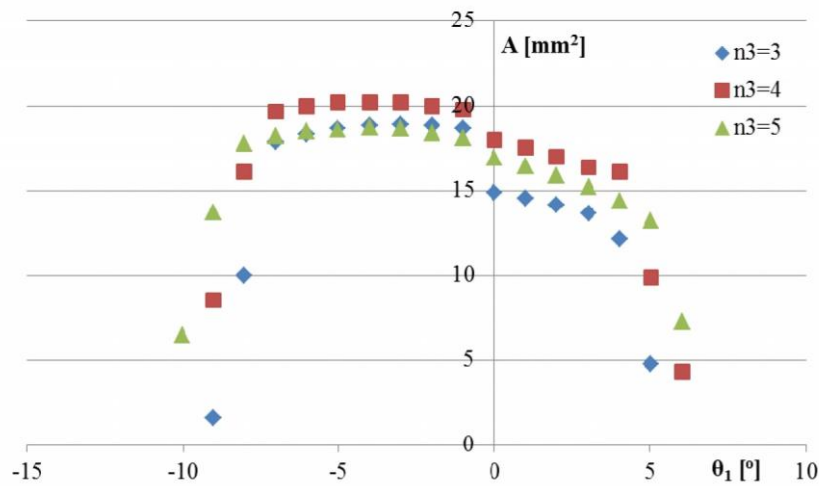


Fig. 6. Influence of exponent n_3 on the gear path of contact
($a = b = 1, n = 2, n_1 = 2, n_2 = 4, m = 2, z = 54$)

When one of the exponents of the trigonometrical terms in supershape equation are varied (Fig. 6), the supershape exhibits important changes in geometry, relative to convexity and symmetry. Therefore, the tooth path of contact follows a peculiar behaviour that could be explained strictly in accordance to the gear geometry.

5. CONCLUSIONS

Most papers published so far, dealing with noncircular gears, are focused on pitch curve and tooth profiles modeling methods or on finding applications for these gears. Few researchers have analyzed and communicated results on the performance of these gears. Taking advantage of the processing and analysis capacity of the latest generation softwares, the authors have conducted further investigations on noncircular gears' behavior, designed in the hypothesis of the driving pitch curve generation, as supershape, with constant pressure angle.

The visualization of the engagement, in both 2D and 3D spaces, allowed the validation of the engagement's accuracy, respectively of the geometrical and kinematical calculations specific to the phases of gear generation process. The three-dimensional investigation of the solid noncircular gears meshing generated important data as regard to the distribution and evolution of the gear path of contact, useful for a better design of the gear geometry and further investigation on noncircular gear behaviour, such as distribution of loads, maximum stress and displacement etc.

ACKNOWLEDGEMENTS

The work of Marius Vasie was supported by Project SOP HRD – EFICIENT 61445/2009.

REFERENCES

1. **Dooner D. B., Seireg A.**, 1995, The kinematic geometry of gearing, John Wiley & Sons.
2. **Mundo D.**, 2006, Geometric design of a planetary gear train with non-circular gears, *Mechanism and machine theory*, vol. 41, pp. 456-472.
3. **Litvin F. L. et al.**, 2008, Design and investigation of gear drives with non-circular gears applied for speed variation and generation of functions, *Comp. Meth. Appl. Mech. Engrg.*, vol. 197, pp. 3783-3802.
4. **Tong S.-H., Yang D. C. H.**, 1998, Generation of identical noncircular pitch curves, *Journal of mechanical design*, vol. 120, pp. 337-341.
5. **Chang S.-L., Tsay C.-B.**, 1998, Computerized tooth profile generation and undercut analysis of noncircular gears manufactured with shaper cutters, *Journal of mechanical design*, vol. 120, pp. 92-99.
6. **Danieli G. A.**, 2000, Analytical description of meshing of constant pressure angle teeth profiles on a variable radius gear and its applications, *Journal of mechanical design*, vol. 122, pp. 203-217;
7. **Li J.-G. et al.**, 2007, Numerical computing method of noncircular gear tooth profiles generated by shaper cutters, *The international journal of advanced manufacturing technology*, vol. 33, pp. 1098-1105.
8. **Gielis J.**, 2003, A generic geometric transformation that unifies a wide range of natural and abstract shapes, *American journal of botany*, pp. 90:333-338.
9. **Vasie M., Andrei L., Mundo D.**, 2011, General model for internal mating centrodes of noncircular gears, *The Annals of Dunarea de Jos University of Galati, Fascicle II, Mathematics, Physics, Theoretical Mechanics*, , Vol. 2, pp. 183-190.
10. **Litvin F.L.**, 1994, Gear geometry and applied theory, Englewood Cliffs, New Jersey, Prentice Hall.
11. **Vasie M.**, 2012, Studies on gears with variable gear ratio, PhD thesis, Dunarea de Jos University of Galati, December.